Materials Transactions, Vol. 43, No. 8 (2002) pp. 1974 to 1978
Special Issue on Bulk Amorphous, Nano-Crystalline and Nano-Quasicrystalline Alloys IV

Thermal Stability and Soft Magnetic Properties of (Fe, Co)–(Nd, Dy)–B Glassy Alloys with High Boron Concentrations

Wei Zhang[1], Yi Long[2], Muneyuki Imafuku[1,*] and Akihisa Inoue[1,3]

[1]*Inoue Superliquid Glass Project, Exploratory Research for Advanced Technology, Japan Science and Technology Corporation, Sendai 982-0807, Japan*
[2]*School of Materials Science and Engineering, University of Science and Technology Beijing, Beijing, 100083, P.R. China*
[3]*Institute for Materials Research, Tohoku University, Sendai 980-8577, Japan*

Fe-based glassy alloys with high boron concentrations in (Fe, Co)–(Nd, Dy)–B system were found to exhibit a large supercooled liquid region (ΔT_x) and good soft magnetic properties. The $Fe_{62}Co_{9.5}Nd_3Dy_{0.5}B_{25}$ glassy alloy with ΔT_x of 56 K exhibits high saturation magnetization (I_s) of 1.41 T, low coercive force (H_c) of 2.6 A/m and large permeability (μ_e) at 1 kHz of 12000. The $Fe_{62}Co_{9.5}Nd_3Dy_{0.5}B_{25}$ glassy alloy rods were produced in the diameter range up to 0.75 mm by copper mold casting. The substitution of 2 at% elements TM (TM = Nb, Ta, Mo and W) for Fe and Co, remarkably increases the ΔT_x and T_g/T_l, leading to an increase in the glass-formation ability (GFA) for $Fe_{60.3}Co_{9.2}Nd_3Dy_{0.5}B_{25}TM_2$. The ΔT_x and T_g/T_l increase from 56 to 87 K and 0.56 to 0.57, respectively, and the glassy alloy rods were produced in the diameter range up to 1.2 mm. The saturation magnetization I_s decreases slightly, while the coercive force H_c remains almost unchanged by the addition of 2 at% TM elements.

(Received February 25, 2002; Accepted April 22, 2002)

Keywords: *iron-based bulk glassy alloy, iron-cobalt-rare earth-boron system, high boron concentration, transition metal, supercooled liquid region, glass-forming ability, soft magnetic properties*

1. Introduction

Since the finding of a melt-spun amorphous Fe–P–C alloy with ferromagnetism in 1967,[1)] Fe- and Co-based magnetic amorphous alloys have attracted increasing interest. Subsequently, (Fe, Co)–P–B and (Fe, Co)–B–Si alloys were reported to exhibit good soft magnetic properties in 1974,[2–4)] followed by (Fe, Co)–(Cr, Mo, W)–C,[5)] (Fe, Co)–(Zr, Hf),[6,7)] and then (Fe, Co)–(Zr, Hf, Nb)–B[8)] alloys in the early 1980s. Among these, the melt-spun (Fe, Co)–B–Si amorphous alloys have been practically used as soft magnetic materials in electronic transformer.[9)] However, those amorphous alloys did not exhibit high glass-formation ability (GFA) and could be produced only at high cooling rates of over 10^5 K/s by melt spinning. As a result, the ribbon sample thickness has been limited to less than about 50 μm.

Glassy alloys with a large supercooled liquid region ΔT_x ($= T_x - T_g$) defined by the difference between glass transition temperature (T_g) and crystallization temperature (T_x) and/or high reduced glass transition temperature T_g/T_l (T_l: liquidus temperature) have high resistance against crystallization, leading to high GFA.[10,11)] In addition, the large deformation and easy working due to its low viscosity and ideal Newtonian flow have been reported to be obtained in the supercooled liquid region. Recently, it has been reported that ferromagnetic Fe- and Co-based glassy alloys with a large supercooled liquid region above 50 K as well as a higher GFA in the Fe–(Al, Ga)–(P, C, B, Si),[12)] Fe–(Co, Ni))–(Zr, Hf, Nb)–B[13)] and Co–Fe–(Zr, Ta, Nb)–B[14)] systems exhibit good soft magnetic properties. The critical thickness of these glassy alloys reaches 2 mm for (Al, Ga)–(P, C, B, Si)[15)] and Fe–(Co, Ni))–(Zr, Hf, Nb)–B systems,[16)] and 1.5 mm for Co–Fe–(Zr, Ta, Nb)–B[17)] system by the copper mold casting method. However, relatively low Fe and Co concentrations lead to a low saturation magnetization. We have searched for a new glassy alloy in (Fe, Co)–RE–B (RE = rear earth elements) system with a B content of 20 at% in which a supercooled liquid region is observed and high saturation magnetization and low coercive force are obtained.[18,19)] The ΔT_x and T_g/T_l for the Fe-based glassy alloys reported up to date are about 45 K and 0.55, respectively, and hence an extremely large GFA cannot be expected.[20,21)] More recently, we have reported that (Fe, Co)–RE–B glassy alloys with high B concentrations about 20 at% exhibit a large ΔT_x above 55 K and good soft magnetic properties.[22)] Subsequently, we have examined the effect of additional transition metals on the thermal stability, glass-formation ability and magnetic properties of those glassy alloys. This paper presents the thermal stability of the supercooled liquid, glass-formation ability and magnetic properties of the $Fe_{87-x}Co_{9.5}Nd_3Dy_{0.5}B_x$ (x = 17.5 to 35) and $Fe_{60.3}Co_{9.2}Nd_3Dy_{0.5}B_{25}TM_2$ (TM = V, Nb, Ta, Cr, Mo and W) glassy alloys. The reasons for the high thermal stability and large glass-formation ability for $Fe_{60.3}Co_{9.2}Nd_3Dy_{0.5}B_{25}TM_2$ glassy alloys are also discussed.

2. Experimental Procedure

Alloy ingots of Fe–Co–Nd–Dy–B–TM (TM = V, Nb, Ta, Cr, Mo and W) were prepared by arc melting from 99.9 to 99.99 mass% purity elemental metals and boron (99.5 mass%) in an argon atmosphere. The ingots were crushed into small pieces, in order to place them into a quartz crucible for melt spinning. Ribbons were produced at a wheel speed of 35 m/s in an argon atmosphere. Bulk samples with length of about 50 mm and rod form with different diameters were produced by injection casting of the molten alloy

*Present address: Advanced Technology Research Laboratories, Nippon Ateel Corporation, Futtsu 293-8511, Japan.

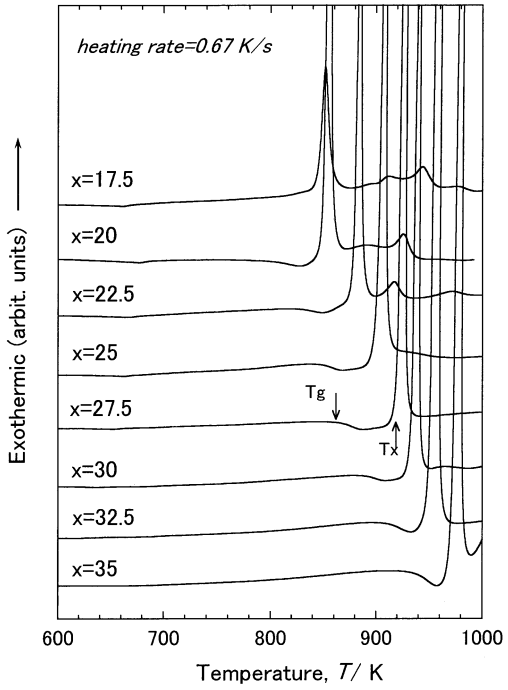

Fig. 1 DSC curves of melt-spun $Fe_{87-x}Co_{9.5}Nd_3Dy_{0.5}B_x$ (x = 17.5 to 35 at%) glassy alloys.

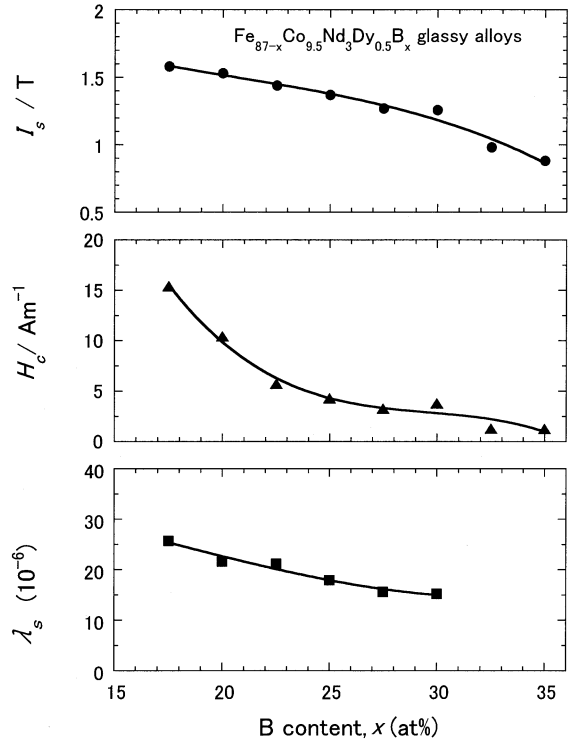

Fig. 2 Saturation magnetization (I_s), coercive force (H_c) and saturated magnetostriction (λ_s) as a function of B content for the melt-spun $Fe_{87-x}Co_{9.5}Nd_3Dy_{0.5}B_x$ (x = 17.5 to 35 at%) glassy alloys.

into copper molds. The structure of the samples was examined by X-ray diffraction (Cu K_α), transmission electron microscopy (TEM) and optical microscopy (MO). Thermal stability was examined by differential scanning calorimetry (DSC) and differential thermal analysis (DTA) under an argon atmosphere at a heating rate of 0.67 K/s, and a cooling rate 0.033 K/s, respectively. The saturation magnetization was measured at room temperature with a vibrating sample magnetometer (VSM) under a maximum applied magnetic field of 670 kA/m. The coercive force was measured with a B-H loop tracer. The saturated magnetostriction was measured by a capacitance method in a maximum applied field of 240 kA/m.

3. Results

The X-ray diffraction patterns indicated that the melt-spun ribbons in the composition range of 0 to 80 at%Co, 0 to 10 at%RE and 15 to 40 at%B were composed of an amorphous single phase. Figure 1 shows the DSC curves of the $Fe_{87-x}Co_{9.5}Nd_3Dy_{0.5}B_x$ (x = 17.5 to 35 at%) amorphous alloys. As marked with the glass transition temperature (T_g) and crystallization temperature (T_x), it is noticed that the glass transition and supercooled liquid region ($\Delta T_x = T_x - T_g$) are observed in the B concentration range of 20 to 35 at%, and the larger ΔT_x values of 56 K and 57 K are obtained at 25 and 27.5 at%B, respectively. We further measured the liquidus temperature (T_l) by DTA. The reduced glass transition temperature (T_g/T_l) is determined to be 0.56 for the $Fe_{87-x}Co_{9.5}Nd_3Dy_{0.5}B_x$ (x = 25 to 30 at%) glassy alloys. The large ΔT_x and high T_g/T_l indicate the possibility that the high GFA is obtained for the alloys containing 25 to 27.5 at%B.[10,11]

Figure 2 shows the saturation magnetization (I_s), coercive force (H_c), and saturated magnetostriction (λ_s) as a function of B content for the melt-spun $Fe_{87-x}Co_{9.5}Nd_3Dy_{0.5}B_x$ (x = 17.5 to 35 at%) glassy alloys. The I_s and H_c values decrease gradually from 1.53 to 1.26 T, and 10.4 to 1.24 A/m, respectively, with increasing B content from 17.5 to 35 at%. The λ_s value also decreases gradually from 21.6×10^{-6} to 15.7×10^{-6} with increasing B content from 17.5 to 30 at%. The I_s, H_c and λ_s values are 1.37 T, 4.27 A/m, and 17.9×10^{-6}, respectively, for 25 at%B glassy alloy in the as-quenched state. After annealing for 600 s at 773 K, the I_s, H_c, λ_s, and the permeability (μ_e) at 1 kHz are 1.41 T, 2.6 A/m, 23.7×10^{-6} and 12000, respectively. From the compositional dependence of thermal stability and magnetic properties, it is concluded that the $Fe_{62}Co_{9.5}Nd_3Dy_{0.5}B_{25}$ glassy alloy has a good combination of higher GFA and better soft magnetic properties. Consequently, subsequent trials on the production of a bulk glassy rod by copper mold casting were made for the $Fe_{62}Co_{9.5}Nd_3Dy_{0.5}B_{25}$ alloy.

The cast $Fe_{62}Co_{9.5}Nd_3Dy_{0.5}B_{25}$ rods with diameters of 0.5 and 0.75 mm were produced. The X-ray diffraction patterns of the bulk alloys consist only of broad peak and no diffraction peak corresponding to a crystalline phase is observed, indicating that a single glassy phase is formed. The hysteresis B-H loops of the cast glassy $Fe_{62}Co_{9.5}Nd_3Dy_{0.5}B_{25}$ rods with diameters of 0.50 and 0.75 mm were measured by VSM. No distinct difference in the hysteresis B-H loops is observed between the bulk samples and the melt-spun glassy ribbon. The bulk glassy $Fe_{62}Co_{9.5}Nd_3Dy_{0.5}B_{25}$ alloy also exhibits high saturation magnetization I_s, *e.g.*, 1.33 T for the ϕ0.5 mm rod and 1.31 T for the ϕ0.75 mm rod, indicating that the glassy alloy rods have nearly the same soft magnetic properties as those for the melt-spun ribbon.

In order to improve further the GFA of the (Fe, Co)–

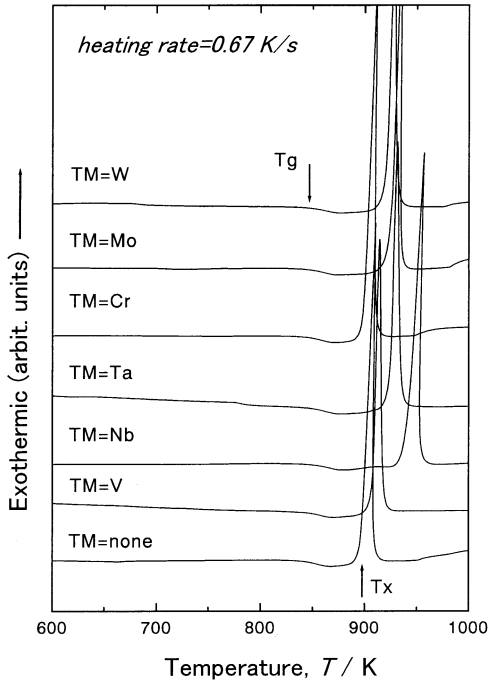

Fig. 3 DSC curves of melt-spun $Fe_{60.3}Co_{9.2}Nd_3Dy_{0.5}B_{25}TM_2$ alloys.

Table 1 Thermal stability of $Fe_{60.3}Co_{9.2}Nd_3Dy_{0.5}B_{25}TM_2$ glassy alloys

Composition	T_g (K)	T_x (K)	ΔT_x (K)	T_l(K)	T_g/T_l
TM = none	844	899	56	1522	0.56
TM = Cr	842	898	56	1541	0.55
TM = Mo	843	924	81	1508	0.56
TM = W	845	921	76	1519	0.56
TM = V	847	907	60	1544	0.55
TM = Nb	850	937	87	1497	0.57
TM = Ta	850	924	74	1494	0.57

(Nd, Dy)–B glassy alloys with high boron concentrations, we have investigated the effects of addition of transition metals TM (TM = V, Nb, Ta, Cr, Mo and W) on the thermal stability, glass-formation ability and magnetic properties of the $Fe_{62}Co_{9.5}Nd_3Dy_{0.5}B_{25}$ glassy alloy. Figure 3 shows DSC curves of the glassy $Fe_{60.3}Co_{9.2}Nd_3Dy_{0.5}B_{25}TM_2$ alloys. As seen in Fig. 3, the T_g remains almost unchanged and the T_x shifts towards higher temperature by the addition of the TM elements, and all the glassy alloys crystallize through a single stage. The ΔT_x exceeds 55 K, and the largest ΔT_x is 87 K for the $Fe_{60.3}Co_{9.2}Nd_3Dy_{0.5}B_{25}Nb_2$ alloy. In addition, we also measured the T_l of the $Fe_{60.3}Co_{9.2}Nd_3Dy_{0.5}B_{25}TM_2$ alloys by DTA. Table 1 lists the thermal stability (T_g, T_x, ΔT_x, T_l and T_g/T_l of the $Fe_{60.3}Co_{9.2}Nd_3Dy_{0.5}B_{25}TM_2$ glassy alloys. From Table 1, it is seen that ΔT_x increases significantly from 56 to 87 K, and the T_l decreases from 1522 to 1494 K with the replacement of 2 at% Fe and Co by elements of Nb, Ta, Mo and W, leading to an increase of T_g/T_l from 0.56 to 0.57. The larger ΔT_x and T_g/T_l for the $Fe_{60.3}Co_{9.2}Nd_3Dy_{0.5}B_{25}TM_2$ alloys (TM = Nb, W, Mo and Ta) indicate that the glass-formation ability of the TM-containing alloys is higher than that of the alloy without TM. The largest ΔT_x of 87 K and high T_g/T_l of 0.57 were obtained

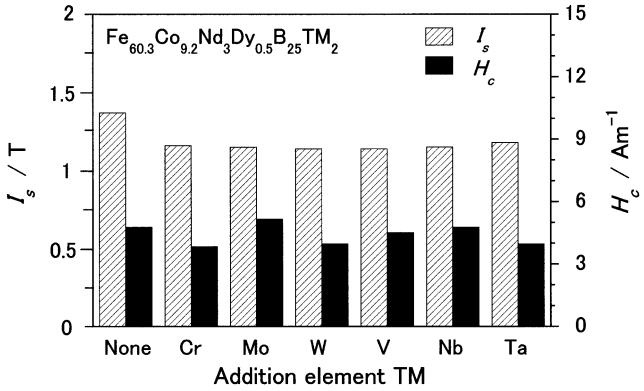

Fig. 4 Saturation magnetization (I_s) and coercive force (H_c) as a function of the transition element TM for the glassy $Fe_{60.3}Co_{9.2}Nd_3Dy_{0.5}B_{25}TM_2$ alloys.

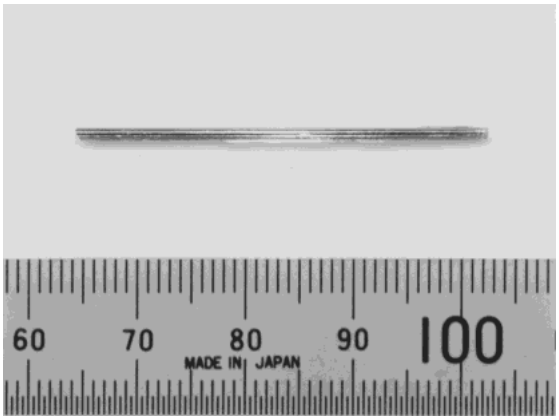

Fig. 5 Outer shape of the cast $Fe_{60.3}Co_{9.2}Nd_3Dy_{0.5}B_{25}Nb_2$ rod with a diameter of 1.2 mm.

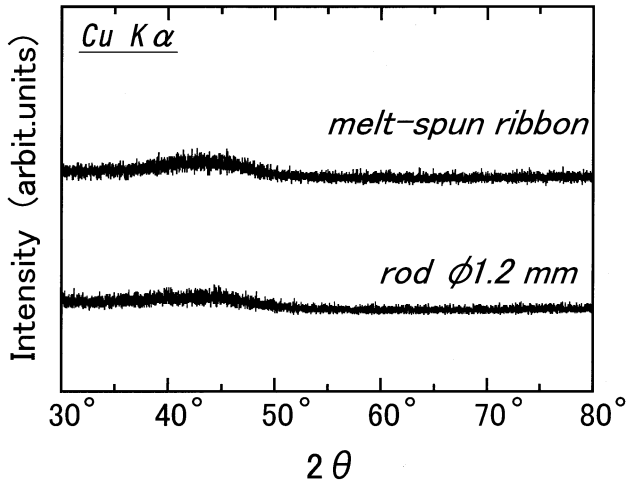

Fig. 6 X-ray diffraction pattern of the cast $Fe_{60.3}Co_{9.2}Nd_3Dy_{0.5}B_{25}Nb_2$ rod with a diameter of 1.2 mm. The data of the melt-spun glassy ribbon with the same composition are also shown for comparison.

for the $Fe_{60.3}Co_{9.2}Nd_3Dy_{0.5}B_{25}Nb_2$ alloy. Figure 4 shows the I_s and H_c of the melt-spun $Fe_{60.3}Co_{9.2}Nd_3Dy_{0.5}B_{25}TM_2$ glassy alloys. The I_s and H_c of the glassy alloys are in the range from 1.13 to 1.19 T and 3.98 to 4.98 A/m, respectively. The H_c remains almost unchanged by the addition of the TM elements. The I_s values are lower than that of the alloy without TM because of the replacement of ferromagnetic elements by the non-ferromagnetic elements of TM.

A cast $Fe_{60.3}Co_{9.2}Nd_3Dy_{0.5}B_{25}Nb_2$ alloy rod with a diam-

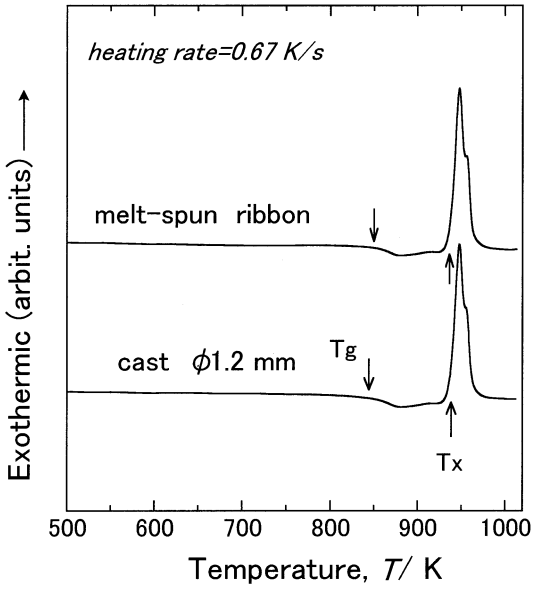

Fig. 7 DSC curves of the cast glassy $Fe_{60.3}Co_{9.2}Nd_3Dy_{0.5}B_{25}Nb_2$ rod with a diameter 1.2 mm. The data of the melt-spun glassy ribbon are also shown for comparison.

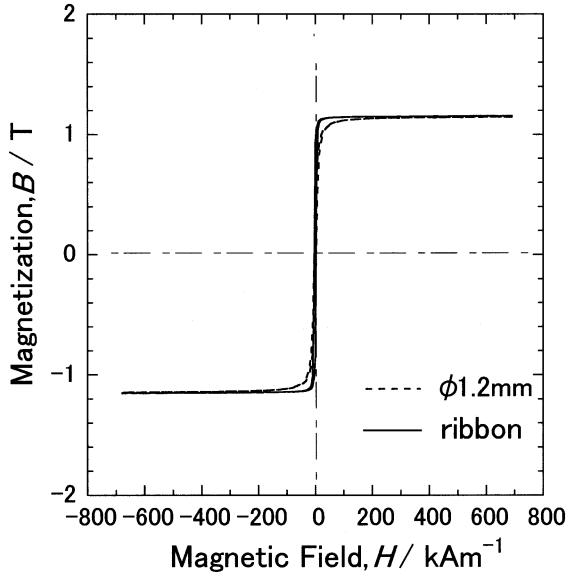

Fig. 8 Hysteresis B-H loops of the cast glassy $Fe_{60.3}Co_{9.2}Nd_3Dy_{0.5}B_{25}Nb_2$ rod with a diameter 1.2 mm. The data of the melt-spun glassy ribbon are also shown for comparison.

eter of 1.2 mm was also produced. Figure 5 shows the outer surface of the cast $Fe_{60.3}Co_{9.2}Nb_3Dy_{0.5}B_{25}Nb_2$ rod. The rod sample has a smooth surface with good metallic luster and no distinct ruggedness due to the precipitation of a crystalline phase is seen on the outer surface. Figure 6 shows an X-ray diffraction pattern of the cast alloy rod, together with the result of the melt-spun glassy alloy ribbon. The X-ray diffraction pattern of the rod sample consists only of a broad peak and no distinct difference is seen between the rod and the melt-spun glassy ribbon samples, indicating the formation of a single glassy phase in the cast rod. The further increase in the rod diameter to 2.0 mm causes the precipitation of crystalline phases. It is therefore concluded that the critical rod diameter for formation of the glassy phase lies between 1.2 and 2.0 mm.

Figure 7 shows the DSC curves of the $Fe_{60.3}Co_{9.2}Nd_3Dy_{0.5}B_{25}Nb_2$ alloy rod with a diameter of 1.2 mm. The data of the melt-spun glassy ribbon are also shown for comparison. The T_g, ΔT_x, and heat of crystallization (ΔH_x) are 849 K, 89 K and 5.99 kJ/mol, respectively, for the rod sample and 850 K, 87 K and 6.14 kJ/mol, respectively, for the ribbon sample. No appreciable difference in T_g, ΔT_x and ΔH_x is seen between these samples. This result also indicates that the bulk alloy has the similar disordered structure as that for the glassy alloy ribbon.

The hysteresis B-H loops of the cast glassy $Fe_{60.3}Co_{9.2}Nd_3Dy_{0.5}B_{25}Nb_2$ rod with a diameter of 1.2 mm are shown in Fig. 8, where the data of the melt-spun glassy ribbon are also shown for comparison. The I_s of the glassy $Fe_{60.3}Co_{9.2}Nd_3Dy_{0.5}B_{25}Nb_2$ rod is 1.15 T which is the same as that of the ribbon sample, and no distinct difference in the hysteresis B-H loops is seen between the cast rod and the melt-spun glassy ribbon. It is reasonable to conclude that the cast bulk glassy sample also has nearly the same soft magnetic properties as those of the melt-spun ribbon on the basis of the similarity in the B-H loops measured by VSM.

4. Discussion

The large supercooled liquid region for the Fe-based (Fe, Co)–(Nd, Dy)–B glassy alloys containing high boron concentrations (20–30 at%) seems to have a strong relation to local atomic structure. The essential structure feature of the (Fe, Co)–RE–B glassy alloys with large ΔT_x was characterized as the formation of the distorted dense random network of trigonal prism-like local units around boron connected with inserted RE.[23–25] The significant difference in atomic sizes among the constituents and the strong chemical affinities of RE–B, RE–Co and RE–Fe pairs contribute to the strengthening of network of the prism, leading to the suppression of the rearrangement of the constituent elements on a long-range scale. Although the prism-like structure was also identified for the amorphous alloys with lower boron contents(18 at% $<$ B), no supercooled liquid region was observed in these alloys. This implies that the network of the prisms is not strong enough to maintain during heating. As for the alloys with higher boron contents(B $>$ 30 at%), the coordination numbers of first nearest neighboring B-(Fe, Co) pairs ($N_{B-(Fe, Co)}$) are much smaller than those in the glassy alloys containing 20–30 at%B,[25] the trigonal prism-like local structure is no longer dominant. This makes the rearrangements of the prisms during crystallization easy.

The substitution of TM (= Nb, Ta, Mo and W) for Fe and Co in the $Fe_{62}Co_{9.5}Nd_3Dy_{0.5}B_{25}$ glassy alloy increases significantly ΔT_x, however, little change in ΔT_x is seen for the substitution of Cr and V (Fig. 3). This result has relation to the local atomic structures of the glassy alloys. The local atomic structures in the $Fe_{70}TM_{10}B_{20}$ glassy alloys (TM = Cr Zr, Nb, Hf and W) with difference ΔT_x were studied.[25–28] The essential features of the atomic structures resemble in these glassy alloys, but differ in the local atomic structure which is a distorted shape of the trigonal prism-like. In the glassy alloys containing TM elements larger than Fe atoms, the prisms show distorted shapes due to a size difference be-

tween TM and Fe. A linear relation between the size difference and ΔT_x, suggests that the difference of ΔT_x is closely related with the difficulty of rearrangements of the prisms during crystallization.[27,28] Similarly, the substitution of larger atomic size TM (= Nb, Ta, Mo and W) for Fe and Co in the $Fe_{62}Co_{9.5}Nd_3Dy_{0.5}B_{25}$ glassy alloy, the difference in atomic sizes between the constituents and the strong chemical affinities of TM–B, TM–Co and TM–Fe pairs contribute to the strengthening of network of the prism, leads to suppression of the rearrangements of the constituent elements on a long-range scale in the present Fe-based glassy alloys.[26–28] On the other hand, the ΔT_x changes little with the substitution of Cr or V element because the atomic sizes of Cr and V are close to those of Fe and Co.

The large GFA of the present Fe-based (Fe, Co)–(Nd, Dy)–B–TM (TM = Nb, Mo, Ta, W) alloy with high boron concentrations is concluded to originate from the high thermal stability of the supercooled liquid against crystallization. The reason for the large ΔT_x and high T_g/T_l for the (Fe, Co)–(Nd, Dy)–B–TM glassy alloy is discussed in the framework of the three component empirical rules[10,11] for the achievement of large GFA. The three component rules are (1) multicomponent systems consisting of more than three elements, (2) significant difference in atomic size above about 12% among the main three constituent elements, and (3) large negative heats of mixing among the elements. The base composition in the present alloys is an Fe–Nd–B system which satisfies the three component rules. The addition of Co, Dy and TM elements is effective for an increase in the degree of the satisfaction of the component rules. That is, the addition of these elements causes the more sequential change in atomic size in the order of Nd > Dy $\gg$ TM $\gg$ Fe > Co $\gg$ B. In the supercooled liquid in which the three component rules are satisfied at higher level, the topological and chemical short-range orderings are enhanced, leading to the formation of a dense random network of trigonal prism-like structure,[23,24] which is the case of the present (Fe, Co)–(Nd, Dy)–B–TM glassy alloys. In addition, the crystallization of the $Fe_{60.3}Co_{9.2}Nd_3Dy_{0.5}B_{25}TM_2$ glassy alloy upon continuous heating takes place from the supercooled liquid through a single exothermic reaction accompanying the simultaneous precipitation of four crystalline phases Fe_3B, $Nd_2Fe_{14}B$, $NdFe_4B_4$ and $Nd_2Fe_{23}B_3$. This crystallization mode also implies the necessity of long-range atomic rearrangements, leading to the high thermal stability of the supercooled liquid against crystallization.[13,16]

5. Summary

We examined the thermal stability of the supercooled liquid, glass-formation ability and magnetic properties of the $Fe_{87-x}Co_{9.5}Nd_3Dy_{0.5}B_x$ (x = 17.5 to 35) and $Fe_{60.3}Co_{9.2}Nd_3Dy_{0.5}B_{25}TM_2$ (TM = V, Nb, Ta, Cr, Mo and W) glassy alloys. The results obtained are summarized as follows.

(1) The supercooled liquid region ΔT_x and reduced glass transition temperature T_g/T_l are 56 K and 0.56, respectively, for the $Fe_{62}Co_{9.5}Nd_3Dy_{0.5}B_{25}$ glassy alloy. The $Fe_{62}Co_{9.5}Nd_3Dy_{0.5}B_{25}$ glassy alloy rods were produced in the diameter range up to 0.75 mm by copper mold casting.

(2) The $Fe_{62}Co_{9.5}Nd_3Dy_{0.5}B_{25}$ glassy alloy annealed at 773 K for 600 s exhibits good soft magnetic properties of 1.41 T for saturation magnetization I_s, 2.6 A/m for coercive force H_c, and 12000 for permeability μ_e at 1 kHz.

(3) The substitution of 2 at% elements TM (= Nb, Ta, Mo and W) for Fe and Co in the $Fe_{62}Co_{9.5}Nd_3Dy_{0.5}B_{25}$ glassy alloy significantly increases T_x and decreases liquidus temperature T_l, leading to the increases in ΔT_x and T_g/T_l from 56 to 87 K and from 0.56 to 0.57, respectively, for the $Fe_{60.3}Co_{9.2}Nd_3Dy_{0.5}B_{25}TM_2$ glassy alloys.

(4) By the substitution of 2 at% elements TM (TM = Cr, V, Nb, Ta, Mo and W) for Fe and Co, the I_s decreases slightly and H_c remains almost unchanged. The I_s and H_c of the glassy $Fe_{60.3}Co_{9.2}Nd_3Dy_{0.5}B_{25}TM_2$ alloys are in the range from 1.13 to 1.19 T and 3.98 to 4.98 A/m, respectively.

(5) The bulk glassy alloy rods were produced in the diameter range up to 1.2 mm by copper mold casting of the $Fe_{60.3}Co_{9.2}Nd_3Dy_{0.5}B_{25}Nb_2$ alloy. The bulk glassy rods also exhibit high I_s of 1.15 T. The magnetic properties are nearly the same as those for the melt-spun glassy ribbon.

REFERENCES

1) P. Duvez and C. H. Lin: J. Appl. Phys. **38** (1967) 4096–4097.
2) R. C. Sherwood, E. M. Gyorgy, H. S. Chen, S. D. Ferris, G. Norman and H. J. Leamy: AIP conf. Proc. **24** (1974) 745–746.
3) T. Egami, P. J. Flanders and C. D. Graham: AIP conf. Proc. **24** (1974) 697–701.
4) H. Fujimori, T. Masumoto, Y. Chi and M. Kikuchi: Jpn. J. Appl. Phys. **13** (1974) 1889–1890.
5) A. Inoue, T. Masumoto, S. Arakawa and T. Iwadachi: *Rapidly Quenched Metals III*, Vol. 1 (Metals Society, 1978) pp. 265–272.
6) M. Nose and T. Masumoto: Sci. Rep. Res. Inst. Tohoku Univ. **A-28** (1980) 232–241.
7) A. Inoue, K. Kobayashi and T. Masumoto: Proc. Conf. On Metallic Glasses, Sci. Tech., Budapest, (1980) 217–222.
8) A. Inoue, K. Kobayashi, J. Kanehira and T. Masumoto: Sci. Rep. Res. Inst. Tohoku Univ. **A-29** (1981) 331–342.
9) T. Masumoto: Bull. Japan Inst. Metals **30** (1991) 375–382.
10) A. Inoue: Mater. Trans., JIM **36** (1995) 866–875.
11) A. Inoue: Acta Mater. **48** (2000) 279–306.
12) A. Inoue and J. S. Gook: Mater. Trans., JIM **36** (1995) 1180–1182.
13) A. Inoue, T. Zhang, T. Itoi and A. Takeuchi: Mater. Trans., JIM **38** (1997) 359–362.
14) T. Itoi and A. Inoue: Mater. Trans., JIM **39** (1998) 762–768.
15) A. Inoue, T. Zhang and A. Takeuchi, A. Murakami and A. Makino: IEEE. Trans. Mag. **32** (1996) 4866–4871.
16) A. Inoue, T. Zhang and A. Takeuchi: Appl. Phys. Lett. **71** (1997) 464–466.
17) T. Itoi and A. Inoue: Mater. Trans., JIM **41** (2000) 1256–1262.
18) W. Zhang and A. Inoue: Mater. Trans., JIM **40** (1999) 78–81.
19) A. Inoue and W. Zhang: J. Appl. Phys. **85** (1999) 4491–4493.
20) W. Zhang and A. Inoue: J. Appl. Phys. **87** (2000) 6122–6124.
21) W. Zhang, M. Matsusita and A. Inoue: Mater. Trans., **41** (2000) 1482–1485.
22) W. Zhang and A. Inoue: Mater. Trans., **42** (2001) 1142–1145.
23) M. Imafuku, K. Yaoita, S. Sato, W. Zhang and A. Inoue: Mater. Trans., JIM **40** (1999) 1144–1148.
24) M. Imafuku, K. Yaoita, S. Sato, W. Zhang, A. Inoue and Y. Waseda: Mater. Sci. Eng. **A304–306** (2001) 660–664.
25) M. Imafuku, W. Zhang and A. Inoue: Trans. Mater. Res. Soc. Jpn. **27** (2002) 7–12.
26) M. Imafuku, S. Sato, T. Nakamura, H. Koshiba, E. Matsubara and A. Inoue: Mat. Res. Soc. Symp. Proc. **664** (2001) L6.1–L6.10.
27) E. Matsubara, S. Sato, M. Imafuku, T. Nakamura, H. Koshiba, A. Inoue and Y. Waseda: Mater. Sci. Eng. **A312** (2001) 136–144.
28) T. Nakamura, E. Matsubara, M. Imafuku, H. Koshiba, A. Inoue and Y. Waseda: Mater. Trans., **42** (2001) 1530–1534.